NEURO

Optimized intravenous Flat Detector CT for non-invasive visualization of intracranial stents: first results

Tobias Struffert · Stephan Kloska · Tobias Engelhorn · Yu Deuerling-Zheng · Sabine Ott · Marc Doelken · Marc Saake · Martin Köhrmann · Arnd Doerfler

Abstract

Objective As stents for treating intracranial atherosclerotic stenosis may develop in-stent re-stenosis (ISR) in up to 30%, follow-up imaging is mandatory. Residual stenosis (RS) is not rare. We evaluated an optimised Flat Detector CT protocol with intravenous contrast material application (i.v. FD-CTA) for non-invasive follow-up.

Methods In 12 patients with intracranial stents, follow-up imaging was performed using i.v. FD-CTA. MPR, subtracted MIP and VRT reconstructions were used to correlate to intra-arterial angiography (DSA). Two neuroradiologists evaluated the images in anonymous consensus reading and calculated the ISR or RS. Correlation coefficients and a Wilcoxon test were used for statistical analysis.

Results In 4 patients, no stenosis was detected. In 6 patients RS and in two cases ISR by intima hyperplasia perfectly visible on MPR reconstructions of i.v. FD-CTA were detected. Wilcoxon's test showed no significant differences between the methods ($p > 0.05$). We found a high correlation with coefficients of the pairs DSA/ FD-CT MIP $r=0.91$, DSA/ FD-CT MPR $r=0.82$ and FD-CT MIP/ FD-CT MPR $r=0.8$.

Conclusion Intravenous FD-CTA could clearly visualise the stent and the lumen, allowing ISR or RS to be recognised. FD-CTA provides a non-invasive depiction of intracranial stents and might replace DSA for non-invasive follow-up imaging.

Keywords Angiography · Flat Detector Computed Tomography · Stent visualization · Intracranial stenosis · Contrast material

T. Struffert (✉) · S. Kloska · T. Engelhorn · S. Ott · M. Doelken ·
M. Saake · A. Doerfler
Department of Neuroradiology,
University of Erlangen-Nuremberg,
Schwabachanlage 6,
91054 Erlangen, Germany
e-mail: tobias.struffert@uk-erlangen.de

Y. Deuerling-Zheng
Siemens AG, Healthcare Sector,
Siemensstr. 1,
91301 Forchheim, Germany

M. Köhrmann
Department of Neurology, University of Erlangen-Nuremberg,
Erlangen, Germany

Introduction

Intracranial stents are increasingly used for treatment of intracranial atherosclerotic disease [1]. Despite a high technical success rate in-stent restenosis (ISR) may occur in up to 30% of these patients [2]. A high rate of these patients will need subsequent treatment of ISR [3]. Also residual stenosis (RS) is not rare [1]. Therefore a careful follow up of these patients is mandatory. The accepted method of choice is conventional digital subtraction angiography (DSA) [4]. This invasive method, however, has the disadvantage of a moderate to high cost and a low but serious complication rate [5]. Therefore, a non-invasive alternative method for assessment of intracranial stents to visualise and evaluate the lumen of the implanted devices is highly desirable.

Recently, Flat-Detector Computed Tomography (FD-CT), as a new computer tomography technique, has been introduced in clinical routine [6]. This new imaging technique provides cross-sectional images acquired with a C-arm system using flat detectors. Most often they are installed as angiographic systems. Flat detectors, compared with multislice computed tomography (MSCT) detectors, have a much smaller detector element size [7]. Therefore

these detectors have the physical features to provide an excellent visualisation in high contrast structures with superior spatial resolution in comparison with MSCT. However, a smaller detector element size receives proportionately lower photon flux, resulting in an inferior contrast resolution [7].

There are some publications concerning the visualisation of the stent itself using FD-CT [8, 9]. The use of intravenous contrast material during FD-CT acquisition to visualise arteries (Flat Detector-Computed Tomography Angiography (FD-CTA) has been reported rarely. There is one report in an animal model demonstrating the feasibility of vessel visualisation of intravenous FD-CTA in comparison to MSCT and DSA [10]. In this study it was shown that despite limited soft tissue resolution of FD-CT a sufficient arterial vessel contrast by intravenous injection was possible. Measurements of vessel diameter showed a high correlation of DSA, MSCT and FD-CT. Recently, a new FD-CT program with dedicated post-processing has shown that intracranial arteries can be visualised in patients with high quality in comparison to MSCT [11]. There is only one report on two patients describing the visualisation of the lumen of intracranial stents after intravenous contrast application using FD-CT [12]. The idea of obtaining FD-CT with intravenous contrast medium application to achieve a MSCT angiography (MS-CTA) like image impression is obvious. The well-known superior spatial resolution might support the visualisation of the stent lumen. Feasibility of sufficient vessel contrast has been shown [10–12]. The purpose of our study was to evaluate the visualisation of intracranial stents and the stent lumen using intravenous FD-CTA with an optimised contrast material application and advanced post-processing in comparison to conventional DSA.

Patients and methods

Ethics committee approval was obtained before this study. According to institutional guidelines, patients treated with intracranial stents are scheduled to follow-up imaging by DSA 6 months after implantation. In addition we performed i.v. FD-CTA in all patients scheduled for control DSA. Written informed consent was obtained in each patient. All patients were investigated by DSA and i.v. FD-CTA in one session.

DSA

Both DSA and i.v. FD-CTA were performed on a biplane flat-detector angiographic system (Axiom Artis dBA, Siemens AG, Healthcare Sector, Forchheim, Germany). Using standard angiographic methods a diagnostic catheter

was used to obtain standard anterior-posterior, lateral and oblique projections (2-D). Angiographic investigation requires about 40 ml of contrast material (Imeron 300, Bracco Imaging, Konstanz, Germany).

Flat Detector computed tomography angiography (i. v. FD-CTA)

Intravenous FD-CTA imaging was performed after removal of the diagnostic catheter and introducer sheath about 25 to 30 min after the last DSA series. The patient was asked to close the eyes and to breathe calmly. A dedicated FD-CT program (DynaCT, Siemens AG, Healthcare Sector, Forchheim, Germany) with a mask run (native) and a second fill run (contrast-enhanced) rotation as described before [11] with an optimised contrast medium application method was used. Data acquisition per run was carried out using the following parameters: acquisition time 10 s per run, 70 kV, 512×512 Matrix, projection on 30×40 cm flat panel size, 200° total angle, 0.8°/Frame, 250 frames total, dose 1.2 μGy/Frame. To control contrast medium influx we used the bolus watching method [11] to visualise a proper time point to start the fill run acquisition as follows (Fig. 1): contrast medium injection is started 5 s after the start of the mask run. The mask run acquisition is completed within 10 s. The C-arm returns to the start position, this requires an interval of 5 s. It can be assumed that within 10 s contrast material injected into a peripheral cubital vein will not reach the cerebral arteries. After the C-arm returns to the start position (10 s after contrast medium injection) then standard 2D-DSA acquisitions are initiated at a rate of two images per second. When contrast opacification of the large arteries is visible the second rotation (fill run) is initiated manually. This method allows acquisition of the fill run with exact contrast material opacification of the arteries. We used 60 mL of contrast material (Imeron 400, Bracco Imaging, Konstanz, Germany) injected into a peripheral cubital vein at a rate of 5 mL/s using a power injector (MEDTRON, Saarbruecken, Germany) followed by a saline chaser (60 ml, injection rate 5 ml/s) [11].

Post-processing and data analysis

Post-processing of the FD-CT data set was performed on a commercially available workstation (syngo XWP, DynaCT, InSpace 3D software, Siemens AG, Healthcare Sector, Forchheim, Germany). The post-processing includes application of system-specific filter algorithms to correct for beam hardening, scattered radiation, truncated projections and ring artefacts. The software allows different algorithms to be used so that reconstructions can be made of the mask run only (analogous to a non-contrast-enhanced CT), and of the fill run separately (analogous to an MSCTA).
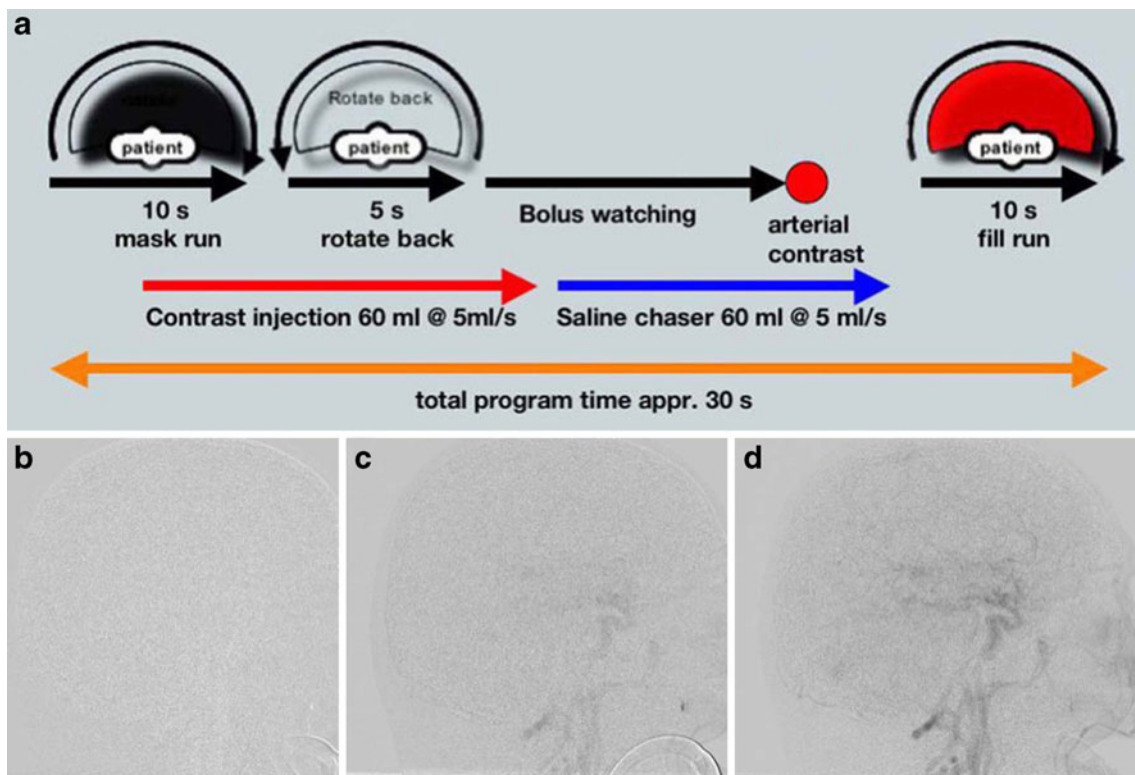
Fig. 1 The acquisition workflow is displayed in (a). The i.v. FD-CT acquisitions starts with the mask run (a, first black arrow). Five seconds later the contrast material injection followed automatically by saline chaser is initiated (red arrow, blue arrow). The C-arm returns to the start position (rotate back, second black arrow). Now bolus watching begins (third black arrow). If opacification of arteries is visible (red circle) the fill run is started manually (fourth black arrow). The procedure requires approximately 30 s depending on the bolus watching phase duration. Bolus watching is displayed in figure b to d. In the first image (b) the contrast material is not obvious. Four seconds later (c) opacification of arteries develops and after 6 seconds arteries are opacified perfectly (d). Then the fill run is initiated

Post-processing of the mask run resulted in 2 volume data sets with a batch of about 370 slices each, 0.1 mm thickness in a 512×512 matrix format. Reconstructions were performed using reconstruction mode "native mask", kernel type "HU", image impression "normal" (reconstruction 1) and "sharp" (reconstruction 2). The first reconstruction was used to have a native image of the stent lumen (MPR reconstruction). The second reconstruction was used to visualise the stent in the volume rendering technique (VRT) as described before [13]. Reconstruction of the fill run resulted in 2 volume data sets and was performed using the reconstruction mode "native fill", kernel type "HU", image impression "normal" (reconstruction 3). This reconstruction was used to have a contrast enhanced image of the stent lumen (MPR reconstruction). Additionally we used reconstruction mode "subtracted", kernel type "EE" and image impression "smooth" (reconstruction 4). This data set was used to perform MIP reconstructions.

We used the 3-D application of the workstation (syngo XWP, 3D software, Siemens AG, Healthcare Sector, Forchheim, Germany) to perform MPR, MIP and VRT reconstructions. MPR reconstructions of the native (reconstruction 1) and contrast-enhanced data set (reconstruction 3) was performed with slice thickness 1 mm and 0.5 mm spacing in axial and sagittal orientation. MIP reconstructions of the subtracted data set were performed with 8-mm thickness and 1-mm spacing (reconstruction 4). We used reconstruction 2 to visualise the stent in VRT as described before [13].

All data were anonymised and transferred to a dedicated workstation (syngo MMWP, Siemens AG Healthcare Sector, Forchheim, Germany). The 2-D DSA and i.v. FD-CTA images of an individual patient were stored separately in random order. The reviewers had the opportunity to review the angiographic series (2-D) subtracted and native with or without filling.

The reviewers were asked two measure the stenosis grade on 2-D DSA series and on MPR and MIP images of i.v. FD-CTA (Fig. 2). The stenosis grade was calculated using the following equation: percentage stenosis = $(1-(D$ stenosis/D normal$)) \times 100$. D stenosis is the diameter at its most severe site. D normal is the diameter of the proximal stent [14] (Fig. 2).

Additional assessment of the stent to recognise RS or ISR was done. On DSA mask images the reviewers were asked to identify the stent and the stent struts to assess if the stent was completely deployed. In FD-CTA the reviewers
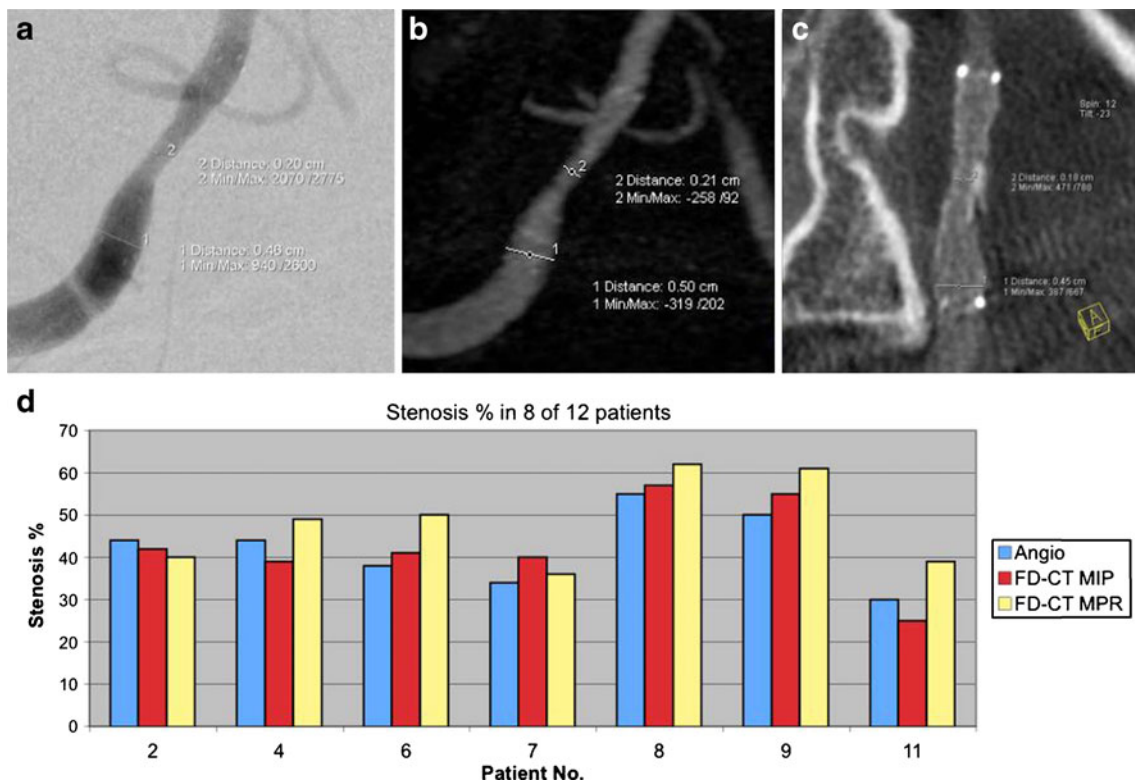
Fig. 2 The measurement method is displayed in **a**, **b** and **c** (patient 2). Stenosis of the V4 segment is visible (**a**, DSA). The MIP reconstruction of the subtracted FD-CTA (**b**) displays the stenosis nicely. MPR reconstruction (**c**) demonstrates perfusion of the lumen of the stent. This case represents RS. The mean stenosis grade in 8 out of 12 patients measured on DSA, MIP and MPR images (**d**) concerning each patient is shown. The measurements are nearly identical in all three techniques

had to assess the opacification of the stent lumen on an ordinal three-point scale (sufficient, poor, no opacification). The VRT images had to be reviewed if the stent was completely open or if narrowing was obvious. Also the reviewers were asked to note any kind of artefacts.

Results

Between October 2009 and March 2010 we included 12 patients, four female and eight male, and the mean age was 64±8 years in this study. All patients gave written informed consent. All patients were treated with an intracranial stent device because of symptomatic intracranial atherosclerotic stenosis and were now routinely scheduled for follow-up imaging an average of 6 months after treatment. At the time of follow up imaging all patients were without symptoms. We used Wingspan Stents (Wingspan™; Boston Scientific/Target, Fremont, CA, USA) in 11 patients and a Pharos Stent (Pharos™, Micrus Endovascular, San Jose, CA, USA) in one patient. Table 1 provides an overview.

In all patients the stents could be recognised on native DSA mask images. Evaluation of the DSA series revealed 100% patency of the treated artery in 4 patients (patient 3, 5, 10, 12). In eight patients stenosis was recognised. In 4 of

these cases, all of them treated for vertebral artery stenosis (patient 1, 2, 7, 11) it was possible to recognise the stent because of the proximal and distal markers but it was impossible to recognise the stent struts. Evaluation if the stent was completely deployed or not was impossible. Consequently differentiation of ISR or RS was impossible (Fig. 3). The other patients (4, 6, 8 and 9) were treated for middle cerebral artery stenosis. In these patients the stents were not superimposed by the skull base so the struts of the stents were visible. In these patients differentiation of ISR or RS was possible. In two patients (8 and 9) the reviewers recognised ISR while two patients (4 and 6) presented with RS. In patients 8 and 9 ISR was recognised because the stent was visible in the native mask as completely deployed while in subtracted images a stenosis was obvious (Fig. 4).

In evaluation of i.v. FD-CTA images the reviewers rated the opacification of the stent lumen to be sufficient in all cases. In all patients the lumen of the stent and the stent struts were perfectly visible. Like in angiography in eight patients a stenosis was obvious. Because of the visibility of the stent struts in all patients it was possible to differentiate ISR or RS in all patients. In patients 8 and 9 material adjacent to the inner stent surface was visible and therefore diagnosed as ISR. In the other patients (1, 2, 4, 6, 7 and 11) the MPR images showed narrowing of the stent and

Table 1 Provides basic demographic information on our patients and the devices used. Results of the measurements are also given

Patient No	Male	Female	Age	Location	Stent	DSA	i.v. FD-CTA	
						Stenosis %	Stenosis MIP %	Stenosis MPR %
1	X		72	V4	WS 4.5X20	38	38	50
2	X		67	V4	WS 4.0X20	44	42	40
3		X	57	M1	WS 3.0X15	0	0	0
4		X	65	M1	WS 2.5X15	44	39	49
5		X	46	C5	WS 4.5X20	0	0	0
6	X		65	M1	WS 3.0X15	38	41	50
7	X		67	V4	WS 4.5X20	34	40	36
8	X		68	M1	WS 3.5X15	55	57	62
9		X	78	M1	WS 2.5X15	50	55	61
10	X		67	M1	WS 3.0X15	0	0	0
11	X		59	V4	WS 3.0X20	30	25	39
12	X		61	V4	Ph 3.5X13	0	0	0

WS Wingspan Stent, *Ph* Pharos Stent

additional VRT reconstructions also revealed incomplete deployment. The MPR and MIP reconstructions were impaired by artefacts of the stent markers at the proximal and distal aperture.

Measurements of the stenosis (8 out of 12 patients) showed a mean stenosis of 41.6% ($\pm$8.3) in angiography, 48.4% ($\pm$9.7) in FD-CT MPR and of 42.1% ($\pm$10.1) in FD-CT MIP. Correlation coefficients were: DSA/ FD-CT MIP 0.91, DSA/ FD-CT MPR 0.82 and FD-CT MIP/ FD-CT MPR 0.8. Wilcoxon's test showed no significant differences between the methods ($p > 0.05$). An overview of the results from each patient with RS or ISR is displayed in Fig. 2.

Discussion

Stent treatment for patients suffering from intracranial atherosclerotic disease is used increasingly [1, 15, 16]. The technical success rate is high but because of the significant ISR rate of about 30% a careful follow up is mandatory. To identify ISR a minimally invasive method should be available. Magnetic resonance angiography in the assessment of ISR is impaired by metal artefacts and therefore not useful [17]. Conventional multislice computed tomography (MSCT) has also been used in the follow-up of intracranial stents. Because of the limited spatial resolution of MSCT it has not developed to become a routine procedure [4, 18]. Stents below 4 mm in diameter cannot be evaluated sufficiently [4]. Therefore, at most institutions DSA is used as a control technique for follow-up but carries the risk of permanent neurological deficits in about 0.5% of all cases [5]. In 2008 Buhk et al. reported that FD-CT after intravenous contrast medium injection should be feasible [12]. In this publication showing the feasibility of this idea

a 20-second rotation time program (DynaCT, Siemens AG, Healthcare Sector, Forchheim, Germany) with a single rotation was used. Contrast material to a volume of 100 ml (Imeron 350) was injected into a cubital vein. The idea to opacify the lumen is obvious because the superior spatial resolution in comparison to MSCT stents can be visualised perfectly with FD-CT [8, 9].

In this article, we present the first results of an optimised FD-CT program to perform control imaging on intracranial stents. A problem of FD-CT programs is the long acquisition time and the fact that bolus tracking as in MS-CTA is not available. Therefore contrast material application is difficult and motion artefacts may disturb the data set. To improve the workflow a kind of bolus tracking and a shorter acquisition time is desirable. Also it seems to be of value to have an additional native data set to post-process subtracted images. This technique is also used increasingly in MS-CTA applications [19]. Therefore we adopted the FD-CT application as described before [11]. The parameters of the contrast material injection protocol in this publication [11] were aiming to reach a steady state to calculate a cerebral blood volume map. This means that veins and dural sinuses needed to be opacified. In this publication a method for determining the contrast medium influx called "bolus watching" has been introduced. We used the identical amount of contrast material but with a higher concentration together with the identical injection rates to those published in Struffert et al. [11]. We changed only the timing, but using the identical bolus watching technique, to detect the arterial phase (Fig. 1). It has been shown in this article that intracranial arteries and veins can be depicted at high quality [11]. We used a dedicated 10 s DynaCT run. We recognised features that demonstrated that this DynaCT run seemed to be appropriate for our purpose. The use of a
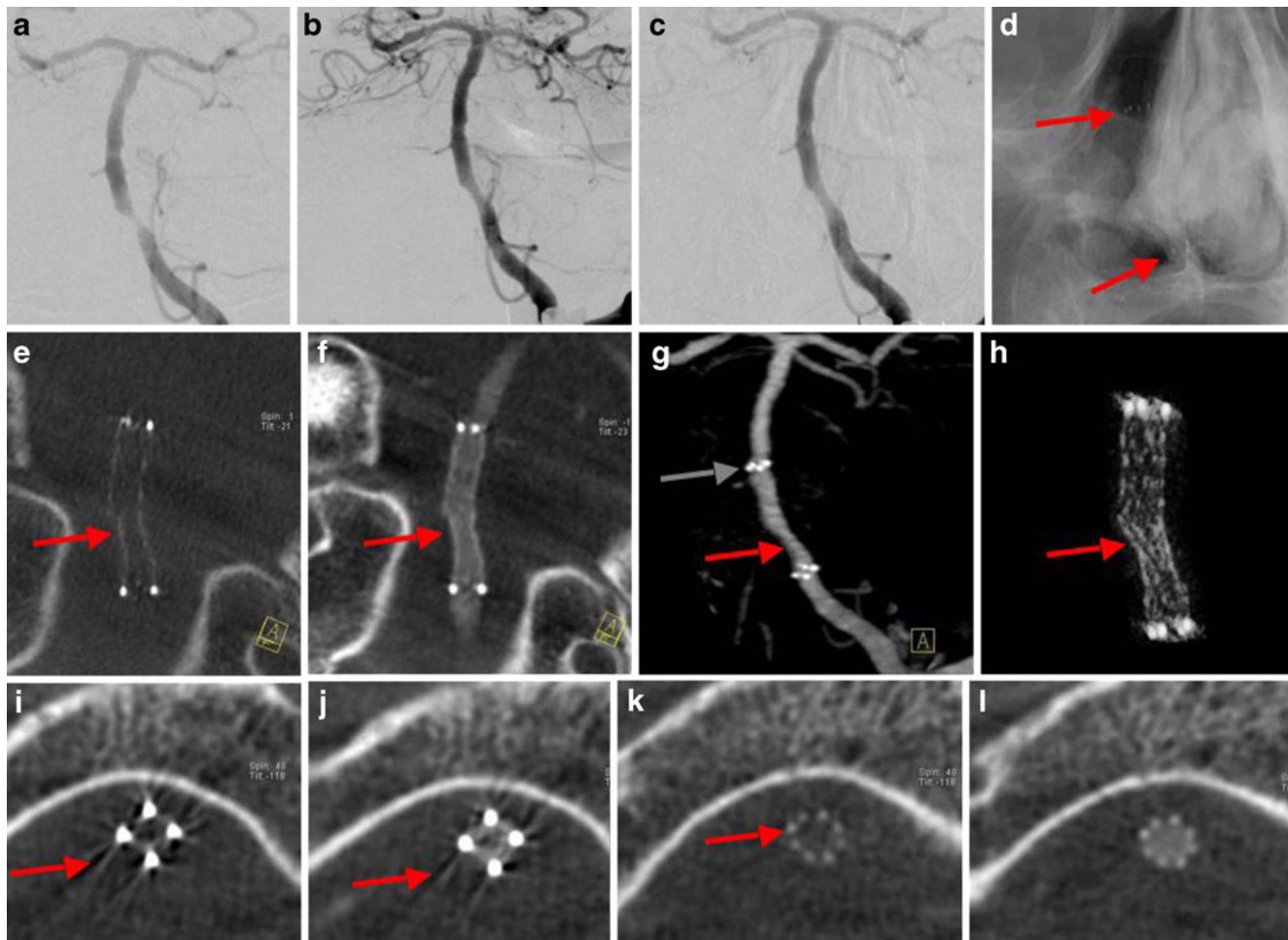
Fig. 3 On DSA images the visibility of the stents is limited. In patient 7 a high grade stenosis (**a**) at the distal V4 level has been treated (**b**), a mild residual stenosis is obvious. Follow-up DSA (**c**) is without any change in comparison. Mask images of the DSA only show the markers (red arrow, **d**). Struts are not visible. FD-CTA evaluation (**e**, native sagittal MPR) clearly shows the residual stenosis (red arrow). Also the VRT reconstruction (**h**, red arrow) shows incomplete deployment of the stent. Contrast-enhanced MPR (**f**) displays the lumen perfused, residual narrowing is obvious (red arrow). In subtracted MIP reconstruction (**g**) the RS is nicely visible (red arrow). Additional artifact of the markers (grey arrow) is to be recognised. In axial MPR reconstructions artefacts of the markers (proximal markers, **i** native, **j** with contrast, **i** and **j** identical slice position) are visible at the aperture of the stent. The struts are perfectly visible (**k**, native images, red arrow). Contrast-enhanced MPR (**l**) nicely demonstrates homogeneous opacification of the stent lumen (K and L identical slice position)

rotation time of 10 s, half of the rotation time used in Buhk et al. [12], may now limit motion artefacts. Additionally it is easier to maintain arterial contrast enhancement over 10 s instead of 20 s. This will decrease the amount of necessary contrast volume. Although it is a program with two acquisitions bolus watching is possible. Our first experience with this new FD-CT application shows that contrast material application using bolus tracking was possible in all patients. We did not have to repeat the acquisition in any of the patients. Contrast opacification of the arteries was sufficient in all patients.

In the follow up of patients treated with intracranial stents it is necessary to recognise ISR [3, 20]. This can only be achieved if we have information on the perfusion of the lumen of the stent and information on the deployment status of the stent device used. Therefore DSA and FD-CT are used in combination in many institutions for follow-up [8, 9]. If stenosis is obvious and the stent is deployed completely an ISR is obvious. If the stent is not completely deployed RS is obvious and additional ISR might be possible. This differentiation seems to be difficult in DSA alone because stent struts can hardly be seen. Especially stents located at the posterior fossa are superimposed by the skull base and only the proximal and distal stent markers are visible. Because of this in our experience stents within the posterior fossa cannot be evaluated by DSA alone, but only in combination with FD-CT.
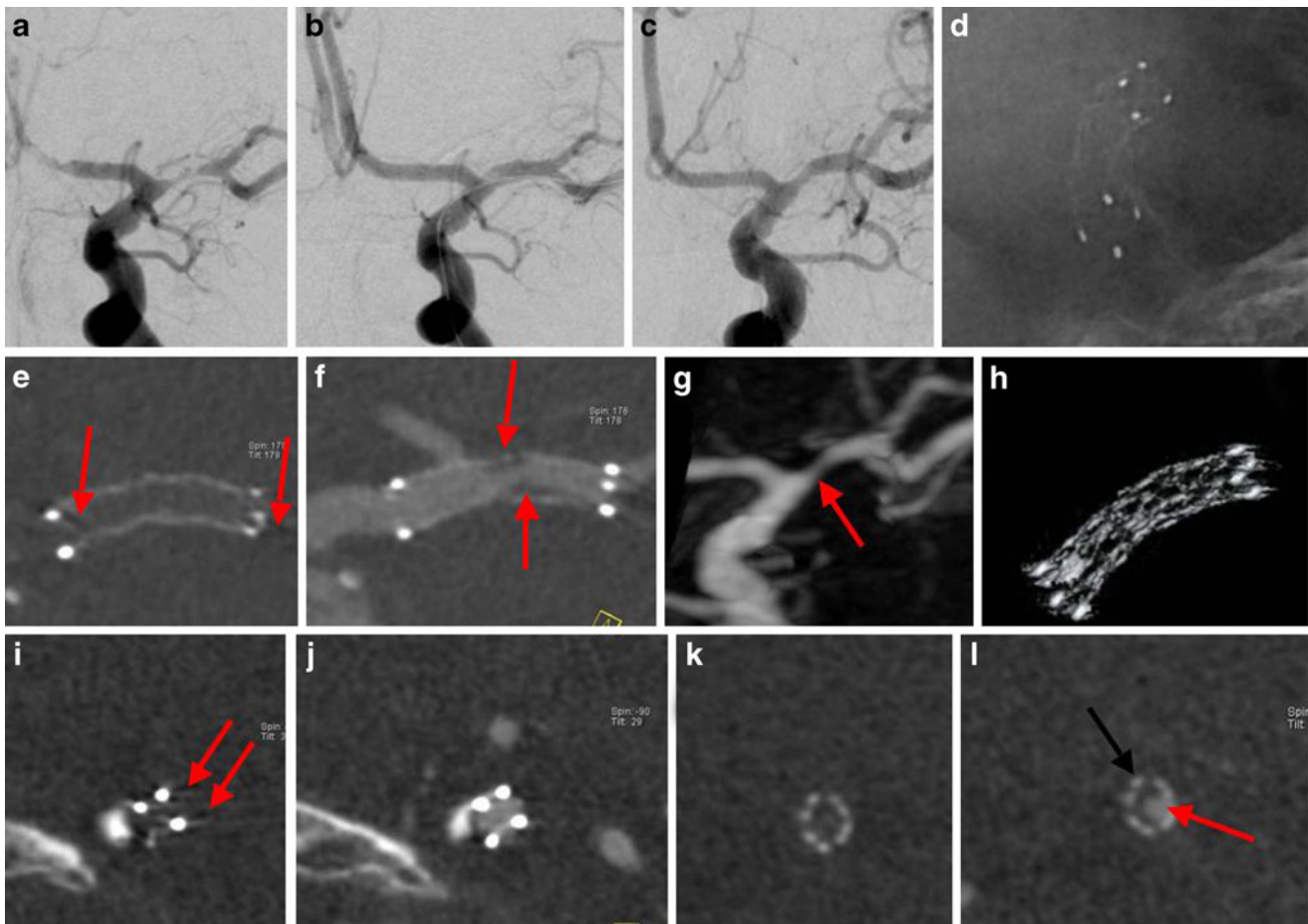
Fig. 4 In patient 8 a high grade MCA stenosis (**a**) was treated (**b**). In follow-up DSA (**c**) a mild stenosis is visible. The struts of the stent can be recognised in native DSA mask image (**d**, oblique view). Therefore ISR is obvious. In i.v. FD-CTA evaluation (**e**, native MPR) and also in VRT reconstruction (**h**) the stent is completely deployed. Notice artefacts of the markers (**e**, red arrows). The contrast-enhanced MPR reconstruction (**f**) nicely shows material (red arrows) adjacent to the inner surface of the stent. This leads to the visualisation of a stenosis in subtracted MIP reconstruction (**g**, red arrow). In axial MPR reconstructions artefacts of the markers (proximal markers, **i** native, **j** with contrast, **i** and **j** identical slice position) are visible at the aperture of the stent (**i**, red arrows), but in this case not as severely as in Fig. 3. Native and contrast-enhanced MPR at the side of stenosis (**k** native, **l** with contrast material) nicely demonstrates material with a half-moon shape adjacent (black arrow) to the inner stent lumen (**k** and **l** identical slice position). The perfused lumen is perfectly visible (red arrow)

The use of an FD-CT program with a native run and a second fill run with contrast material may enhance improved post-processing possibilities. In comparison with DSA the FD-CT program used offers the advantage of visualising the stent, the lumen (native run) and the perfused stent lumen (fill run). The reviewers noticed good opacification of the arteries and the stent lumen. The stent struts were visible in all patients, so recognition of RS was easy in MPR but also in VRT images of the stents. In MPR images before and after contrast material injection the perfused lumen of the stent was clearly visible. Therefore in two patients ISR was easy to recognise. It seems to be of great advantage of i.v. FD-CTA that different reconstructions allow the stent to be investigated for different aspects to recognise in-stent changes. Here i.v. FD-CTA seems to be superior to DSA.

Our measurements of the stenosis grade showed that the mean stenosis grade was within about 8% with a wide overlapping standard deviation. A high correlation of the three different methods was obvious. Wilcoxon's test revealed no significant differences between the measurements. Thus, regarding the recognition of a stenosis itself DSA and i.v. FD-CTA seem to be equal.

In a comparison of DSA and our FD-CT program with advanced post-processing it is possible to examine a patient within 10 min. Hospitalisation is not necessary. The examination harbours the risks of contrast material application, but the typical risks of DSA (neurological complications on the puncture side) cannot occur.

Our study has shortcomings. The number of patients is limited, but sufficient to show feasibility and to provide a

good impression of i.v. FD-CTA image quality. We investigated patients with DSA and i.v. FD-CT exclusively, so we cannot comment on a comparison with MSCT, ultrasound or MRI. The VRT reconstruction that we usually obtain routinely by a 20-second program in follow-up to visualise the stent itself [9] seems to be of better quality in comparison to the 10-second run used in our study (subjective impression of the reviewers). But the VRT images are of sufficient quality to assess the deployment status of the stent.

Intravenous FD-CTA is a promising new technique. Despite beam hardening artefacts of the stent markers assessment of the stent lumen was possible in all patients. In future post-processing techniques should try to reduce these as much as possible [21] to improve image quality. If these artefacts can be reduced this new imaging technology with advanced post-processing may have the possibility to serve as a control imaging technique not only for stents but additionally for intracranial aneurysms or other entities treated via an endovascular route and may replace intra-arterial control assessment [22].

Conclusion

In this article, we present an i.v. FD-CT program with an optimised work-flow and post-processing with the capability to visualise intracranial stents. In comparison with DSA the evaluation of the stenosis grade was identical. Intravenous FD-CTA seems to be superior in the characterisation of RS and ISR in comparison to DSA. The reconstructions clearly visualised the stent lumen, allowing distinguishing between ISR and RS. Therefore i.v. FD-CTA provides a non-invasive depiction of intracranial stents and may serve as a non-invasive alternative tool to DSA for follow-up imaging. Further evaluation is mandatory before i.v. FD-CTA may replace DSA in these patients.

References

1. Bose A, Hartmann M, Henkes H, Liu HM, Teng MM, Szikora I et al (2007) A novel, self-expanding, nitinol stent in medically refractory intracranial atherosclerotic stenoses: the Wingspan study. Stroke 38:1531–1537
2. Levy EI, Turk AS, Albuquerque FC, Niemann DB, Aagaard-Kienitz B, Pride L et al (2007) Wingspan in-stent restenosis and thrombosis: incidence, clinical presentation, and management. Neurosurgery 61:644–650
3. Fiorella DJ, Levy EI, Turk AS, Albuquerque FC, Pride GL Jr, Woo HH et al (2009) Target lesion revascularization after wingspan: assessment of safety and durability. Stroke 40:106–110
4. Trossbach M, Hartmann M, Braun C, Sartor K, Hähnel S (2004) Small vessel stents for intracranial angioplasty: in vitro evaluation of in-stent stenoses using CT angiography. Neuroradiology 46:459–463
5. Willinsky RA, Taylor SM, TerBrugge K, Farb RI, Tomlinson G, Montanera W (2003) Neurologic complications of cerebral angiography: prospective analysis of 2, 899 procedures and review of the literature. Radiology 227:522–528
6. Kalender WA, Kyriakou Y (2007) Flat-detector computed tomography (FD-CT). Eur Radiol 17:2767–2779
7. Kalender WA (2003) The use of flat-panel detectors for CT imaging. Radiologe 43:379–387
8. Benndorf G, Strother CM, Claus B, Naeini R, Morsi H, Klucznik R et al (2005) Angiographic CT in cerebrovascular stenting. AJNR Am J Neuroradiol 26:1813–1818
9. Benndorf G, Klucznik RP, Strother CM (2006) Images in cardiovascular medicine: angiographic computed tomography for imaging of underdeployed intracranial stent. Circulation 114:e499–500
10. Struffert T, Doelken M, Adamek E, Schwarz M, Engelhorn T, Kloska S et al (2010) Flat-detector computed tomography with intravenous contrast material application in experimental aneurysms: comparison with multislice CT and conventional angiography. Acta Radiol 51:431–437
11. Struffert T, Deuerling-Zheng Y, Kloska S, Engelhorn T, Strother CM, Kalender WA et al (2010) A Flat Detector CT in the evaluation of brain parenchyma, intracranial vasculature, and cerebral blood volume: a pilot study in patients with acute symptoms of cerebral ischemia. AJNR Am J Neuroradiol. doi:10.3174/ajnr.A2083
12. Buhk JH, Lingor P, Knauth M (2008) Angiographic CT with intravenous administration of contrast medium is a noninvasive option for follow-up after intracranial stenting. Neuroradiology 50:349–354
13. Benndorf G, Claus B, Strother CM, Chang L, Klucznik RP (2006) Increased cell opening and prolapse of struts of a neuroform stent in curved vasculature: value of angiographic computed tomography: technical case report. Neurosurgery 4(Suppl 2):ONS-E380, discussion ONS-E380
14. Nguyen-Huynh MN, Wintermark M, English J (2008) How accurate is CT angiography in evaluating intracranial atherosclerotic disease? Stroke 39:1184–1188
15. SSYLVIA Study Investigators (2004) Stenting of Symptomatic Atherosclerotic Lesions in the Vertebral or Intracranial Arteries (SSYLVIA): study results. Stroke 35:1388–1392
16. Hartmann M, Jansen O (2005) Angioplasty and stenting of intracranial stenosis. Curr Opin Neurol 18:39–45
17. Prabhakaran S, Warrior L, Wells KR, Jhaveri MD, Chen M, Lopes DK (2009) The utility of quantitative magnetic resonance angiography in the assessment of intracranial in-stent stenosis. Stroke 40:991–993
18. Turk AS, Rowley HA, Niemann DB, Fiorella D, Aagaard-Kienitz B, Pulfer K et al (2007) CT angiographic appearance of in-stent restenosis of intracranial arteries treated with the Wingspan stent. AJNR Am J Neuroradiol 28:1752–1754
19. Buerke B, Wittkamp G, Seifarth H, Heindel W, Kloska SP (2009) Dual-energy CTA with bone removal for transcranial arteries: intraindividual comparison with standard CTA without bone removal and TOF-MRA. Acad Radiol 16:1348–1355
20. Albuquerque FC, Levy EI, Turk AS, Niemann DB, Aagaard-Kienitz B, Pride GL Jr (2008) Angiographic patterns of Wingspan in-stent restenosis. Neurosurgery 63:23–27
21. Prell D, Kyriakou Y, Struffert T, Dörfler A, Kalender WA (2010) Metal artifact reduction for clipping and coiling in interventional C-arm CT. AJNR Am J Neuroradiol 31:634–649
22. Buhk JH, Kallenberg K, Mohr A, Dechent P, Knauth M (2009) Evaluation of angiographic computed tomography in the follow-up after endovascular treatment of cerebral aneurysms–a comparative study with DSA and TOF-MRA. Eur Radiol 19:430–6